A NEW TECHNIQUE FOR BLIND SOURCE SEPARATION USING SUBBAND SUBSPACE ANALYSIS IN CORRELATED MULTICHANNEL SIGNAL ENVIRONMENTS

Karim G. Oweiss, David J. Anderson

Electrical Eng. & Computer Sc. Dept., University of Michigan, Ann Arbor 48109, USA

ABSTRACT

We investigate a new framework for the problem of blind source identification in multichannel signal processing. Inspired by a neurophysiological data environment, where an array of closely spaced recording electrodes is surrounded by multiple neural cell sources [1], significant spatial correlation of source signals motivated the need for an efficient technique for reliable multichannel blind source identification. In a previous work [2], we adopted a new approach for noise suppression based on thresholding an Array Discrete Wavelet Transform (ADWT) representation of the multichannel data. We extend the work in [2] to identify sources from the observation mixtures. The technique relies on separating sources with highest spatial energy distribution in each frequency subband spanned by the corresponding wavelet basis. Accordingly, the best basis selection criterion we propose benefits from the additional degree of freedom offered by the space domain. The amplitude and shift invariance properties revealed by this technique make it very efficient to track spatial source variations sometimes encountered in multichannel neural recordings. Results from multichannel multiunit neural data are presented and the overall performance is evaluated.

1. INTRODUCTION

Multichannel signal processing aims at fusing data collected at several sensors in order to carry out an estimation task of signal sources. Generally speaking, the parameters to be estimated reveal important information characterizing the sources from which the data is observed. Among the numerous biomedical applications of array processing [3-4], neurophysiological recordings of neural cells in the brain using an array of closely spaced electrodes has received much attention in the last decade due to recent advances in microprobe fabrication and packaging [1]. Nevertheless, the need for efficient array processing algorithms to process the vast amount of information obtained in the nervous system continues to emerge as more data becomes feasible to acquire. In a previous work [2], we showed that it is possible to efficiently suppress noise processes in multichannel recordings with an array denoising algorithm with the minimal number of assumptions governing the underlying signal and noise processes. In this work, the primary focus is on the source separation problem. We approach the problem from a new Multi-Resolution Subspace Analysis (MRSA) framework. In the next section, we describe the relevant DWT theory and focus on important properties revealed by applying MRSA to the transform domain.

*This work was supported by NIH under grant number P41RR09754.

2. MULTIRESOLUTION ANALYSIS

2.1. The Discrete Wavelet Transform

The transform consists of an atomic decomposition representing the discrete signal in $l^2(Z)$ successively into different frequency bands in terms of shifted and dilated versions of a prototype bandpass wavelet function $\psi(n)$ and a low pass scaling function $\phi(n)$. An orthonormal basis is formed with a special choice of the wavelet and scaling functions [5].The basis functions can be obtained from the prototype wavelet and scaling functions as

$$\psi_{jk}(n) = 2^{-j/2}\psi(2^{-j}n-k)$$
$$j=1,2,\ldots L,\ k=1,2,\ldots,N \quad (1)$$
$$\phi_{jk}(n) = 2^{-j/2}\phi(2^{-j}n-k)$$
$$j=1,2,\ldots L,\ k=1,2,\ldots,N \quad (2)$$

The *single* channel data vector denoted by $\boldsymbol{x} = (x[1], x[2], ..., x[N])$ will accordingly be represented by

$$\boldsymbol{x} = \sum_k a_{L,k}\phi_{Lk}(n) \ + \ \sum_{j=1}^{L}\sum_k d_{j,k}\psi_{jk}(n) \quad (3)$$

where the *approximation* coefficients and the *details* coefficients, comprising the DWT at level j, are respectively, given by

$$\boldsymbol{a}_j = \langle \boldsymbol{x}, \phi_j \rangle \quad (4)$$
$$\boldsymbol{d}_j = \langle \boldsymbol{x}, \psi_j \rangle \quad (5)$$

where $\langle . \rangle$ denotes a dot product, and L denotes the number of decomposition levels desired in the multiresolution analysis.

2.2. The Discrete Wavelet Packet Transform

The DWPT can be best understood using a binary tree structure, where the root node constitutes the signal level (level 0), and each level constitutes successive decomposition of the parent node to its children using equations (3-5). This amounts to an overcomplete signal representation. Details of the DWPT will be omitted here and can be found in [6].

Best signal representation can be obtained by pruning the wavelet packet tree according to a *best basis* selection criterion. By associating a cost function to each node of the tree and comparing the parent node's cost to its children's cost, a node is further split if it yields a lower cost than its children. Many best basis selection criteria have been proposed in the literature based on single channel data models [7-8].

3. ARRAY BEST BASIS SOURCE SEPARATION (ABBSS)

The ABBSS technique relies on applying signal subspace analysis to the transformed data matrix obtained by applying an undecimated DWPT to each of the M channels data vectors. We define a new best basis selection criterion and show that the obtained wavelet packet tree characterizes each source describing its spectral energy distribution across frequency subbands.

3.1. Blind Source Model

The conventional model for blind source identification in array processing [3] assumes the presence of P sources impinging on an M channel array over the N snapshots, and can be expressed as

$$\boldsymbol{X} = \boldsymbol{A}\boldsymbol{S} + \boldsymbol{Z} \tag{6}$$

where $\boldsymbol{X}$ is the MxN matrix of observations. The MxP matrix $\boldsymbol{A}$ denotes the "mixing matrix" (also known as steering matrix adhering to the Direction Of Arrival (DOA) estimation literature), $\boldsymbol{S}$ denotes the PxN signal matrix that we which to estimate, and $\boldsymbol{Z}$ denotes an MxN matrix of *iid* additive noise component independent of the source signals. Unlike most of the existing array models where the noise is assumed both temporally and spatially white, we assume the most general case where the noise is spatially and temporally correlated [9].

Transforming both sides of (6) with an undecimated DWPT matrix operator $\boldsymbol{W}$, we can write, for the j^{th} node (subband), the MxN Array DWPT (ADWPT) of $\boldsymbol{X}$

$$\boldsymbol{W}_x^j = \boldsymbol{A}_j \boldsymbol{W}_s^j + \boldsymbol{W}_z^j \tag{7}$$

We note here that the mixing matrix is indexed by j, to emphasize the hypothesis that the sources are mixed differently in each subband according to their respective spectral distribution. This will constitute a key feature in the best basis selection criteria that we'll describe later. The ML estimate of the spatial covariance matrix of $\boldsymbol{W}_x^j$ in (7) can be expressed as

$$\boldsymbol{R}_x^j = \boldsymbol{E}[\, \boldsymbol{W}_x^j . \boldsymbol{W}_x^{j^T} \,] \cong \frac{1}{N} \sum_{k=1}^{N} \boldsymbol{w}_{xk}^j \, \boldsymbol{w}_{xk}^{j^T} \tag{8}$$

where $\boldsymbol{w}_{xk}^j$ denotes the Mx1 DWPT coefficient vector of the j^{th} node (subband) at the k^{th} translation index. According to our model, the noise process is not spatially white. This implies that in the j^{th} subband, $\boldsymbol{R}_x^j$ will not be diagonal. Using subspace analysis techniques [10], we can express $\boldsymbol{R}_x^j$ as

$$\boldsymbol{R}_x^j = \boldsymbol{U}_x^j . \boldsymbol{D}_x^j . \boldsymbol{U}_x^{j^H} \tag{9}$$

The matrix $\boldsymbol{U}_x^{j^H}$ is a whitening matrix that diagonalizes $\boldsymbol{R}_x^j$. The transformation

$$\widetilde{\boldsymbol{W}}_x^j = \boldsymbol{U}_x^{j^H} . \boldsymbol{W}_x^j \tag{10}$$

whitens the ADWPT matrix $\boldsymbol{W}_x^j$. Substituting from (7) in (10), the j^{th} whitened wavelet packet can be expressed as

$$\widetilde{\boldsymbol{W}}_x^j = \boldsymbol{U}_x^{j^H} . \boldsymbol{A}_j . \boldsymbol{W}_s^j \quad + \quad \widetilde{\boldsymbol{W}}_z^j \tag{11}$$

where $\widetilde{\boldsymbol{W}}_z^j$ denotes the whitened wavelet noise packet in the j^{th} subband.

Using wavelet thresholding techniques for noise cancellation [11], and denoting the thresholding matrix operator by $\boldsymbol{H}_j$, shrinking or setting to zeros the low amplitude coefficients in (11) can be performed to obtain the *noise free* wavelet expansion

$$\overline{\boldsymbol{W}}_x^j = \boldsymbol{H}_j . \widetilde{\boldsymbol{W}}_x^j \tag{12}$$

Since wavelet observations are decorrelated in (10), the denoising threshold can be estimated according to [11]. Substituting for $\widetilde{\boldsymbol{W}}_x^j$ from (11)

$$\overline{\boldsymbol{W}}_x^j = \boldsymbol{U}_x^{j^H} . \boldsymbol{A}_j . \boldsymbol{W}_s^j \tag{13}$$

or simply,

$$\overline{\boldsymbol{W}}_x^j = \boldsymbol{V}_x^j . \boldsymbol{W}_s^j \tag{14}$$

Having reached this stage, the problem reduces to the determination of the *M*x*P* unitary matrix $\boldsymbol{V}_x^j$. This is easily determined from second order statistics as in [12] or higher order statistics as in [13]. A closed form expression for an estimate of the mixing matrix $\boldsymbol{A}_j$ can be expressed as

$$\begin{aligned} \boldsymbol{A}_j &= (\boldsymbol{U}_x^{j\,H})^{-1}.\boldsymbol{V}_x^j \\ &= \boldsymbol{U}_x^j.\boldsymbol{V}_x^j \end{aligned} \tag{15}$$

3.2. Source Identification

Recall that in a neural cell population environment, neural sources fire spikes that have significant correlation in waveform shapes. Accordingly, their spectral distributions overlap to a high extent. Thus the assumption of a diagonal signal covariance matrix $\boldsymbol{R}_s$ does not hold in general. However, in the wavelet domain, the overall spectrum is partitioned into smaller subbands, yielding *some* subbands, or equivalently tree *nodes*, where each source has a higher spectral energy representation than any of the other sources. Mathematically, this amounts to computing mixing matrices $\boldsymbol{A}_j$'s and selecting the ones under the constraint that each has rank close to one. Equivalently, subband eigenvalue/eigenvector pairs having the strongest mode (highest eigenvalue) will be selected as the ones best describing the signal source. Nodes in the tree that best represent each source can be selected to uniquely identify the spectral distribution of the source. Mathematically, by denoting the best basis selection operator by $\boldsymbol{B}_j$

$$\boldsymbol{B}_j = \begin{cases} 1 & \boldsymbol{A}_j \text{ has rank close to one} \\ 0 & \text{otherwise} \end{cases} \tag{16}$$

then,

$$\hat{\boldsymbol{W}}_s^j = (\boldsymbol{B}_j \{\boldsymbol{V}_x^j\})^{-1}.\overline{\boldsymbol{W}}_x^j \tag{17}$$

The signal matrix estimate can be obtained by inverse wavelet transformation using the DWPT inverse operator $\boldsymbol{W}^{-1}$

$$\boldsymbol{S} = \boldsymbol{W}^{-1}\{\hat{\boldsymbol{W}}_s\} \tag{18}$$

4. RESULTS

The aforementioned technique was applied to a multichannel neural recording obtained from a Dorsal Cochlear Nucleus (DCN) of adult guinea pigs using a silicon substrate microprobe fabricated at the University of Michigan Center for Neural Communication Technology where this work was developed. Raw data from a 16-channel probe was acquired and a 10 *msec* 4-channel subset of the data is shown in Fig.1. The blind source identification task was required to identify different spike shapes from 3 different neural cells observed on the 4-channel subarray. Fig. 2 illustrates 3 different spike shapes detected in Fig.1-b, and the corresponding best wavelet packet trees. Each identified neural source was assigned a code word according to the path followed in the tree in a top-down left-right labeling scheme (a 0 corrpesonds to a terminal node and 1 otherwise). Fig. 3 shows the average of λ_{max} versus tree node index, where the tree in this case is labeled linearly increasing in top/left to bottom/right order with node 0 being the tree root (signal level). It can be noticed that all sources share the upper part of the tree (left section of the Fig.3), typically corresponding to spectral energy distribution in the first few coarse subbands. As we progress deeper along the tree (to the right), subbands become finer in frequency (coarser in time) permitting separation of sources (middle and bottom subbands).

5. CONCLUSION

The methodology that we have introduced in this work has a number of attractive features. *First*, in contrast to blind source separation approaches using second-order and/or high order statistics, the proposed approach allows the separation of sources with overlapping spectral shape but with different spatial time scale signatures. *Second*, the effects of spreading the noise power using the wavelet transform while localizing the source energy in different frequency subbands amounts to increasing the robustness of the proposed approach with respect to noise. *Third*, the identification method is shift invariant since we use an undecimated DWPT. *Fourth*, spatial variation of the source signals sometimes encountered in this signal environment [14] is accounted for by the spatial weighting inherent in the selection criterion hence the amplitude invariance property. If the sources were temporally uncorrelated, their covariance matrix will have a diagonal structure and this method will guarantee separation of all sources. In the more general case where the sources are correlated, this method offers a more reliable way of best basis selection. *Fifth*, the technique works under the assumption that sources are statistically independent but correlated unlike most blind source identification techniques where the lack of information about the channels is compensated for by assuming that the source signals are statistically independent and uncorrelated. *Sixth,* the compression ability of the DWT makes it very attractive for economic hardware implementation.

7. REFERENCES

[1] Drake K.L., et. al., "Performance of planar multisite microprobes in recording extracellular activity," *IEEE Trans. on BME*., Vol. 35: pp. 719-732, 1988

[2] Oweiss K.G. and Anderson D.J. "A New Approach to Array Denoising," *Proceedings of the 34th Asilomar Conference on Signals, Systems and Computers, Pacific Grove,* October 2000.

[3] Krim H. and Viberg M., " Two decades of array signal processing research," *IEEE SP magazine*: pp. 67-94, July 1996.

[4] Metin A.: *Editor*, *Time frequency and wavelets in biomedical signal processing,* Piscataway, NJ: IEEE Press, 1998

[5] Daubechies I., *Ten lectures on Wavelets*. Philadelphia, PA: SIAM, 1992.

[6] Mallat S., *A Wavelet Tour of Signal Processing*, Academic Press, 2nd edition, pp. 413: 1999.

[7] Krim H. et.al., "Best basis algorithm for signal enhancement," in IEEE ICASSP'95: pp. 1561-1564, May 1995

[8] Coifman R., Wickerhauser M., "Entropy based algorithms for best basis selection," *IEEE Trans. on IT*, vol. 38: pp. 713-718, March 1992

[9] Rao A.M. and Jones D.L., "A Denoising Approach to Multisensor Signal Estimation," *IEEE Trans. on SP*, vol. 48, No. 5, 2000.

[10] Moon T.K. and Stirling W. C., *Mathematical Methods and Algorithms for Signal Processing,* Prentice Hall, New Jersey, *1*st edition, 2000.

[11] Donoho D.L. and Johnstone I., "Adapting to unknown smoothness via wavelet shrinkage," *JASA*, vol. 90, pp.1200-1223, 1995.

[12] Lindgren U. and Broman H., "Source separation using a criterion based on second order statistics," *IEEE Trans. on SP*, vol. 46, no.7: pp. 1837-1850, July 1998

[13] Yellin D. and Weinstein E., "Multichannel signal separation: Methods and analysis," *IEEE Trans. on SP*, vol.44: pp. 106-118, 1996

[14] Harris K. D., et. al., "Accuracy of Tetrode spike separation as determined by simultaneous intracellular and extracellular measurements," *J. Neurophysiology* 84: pp. 401-414, 2000.

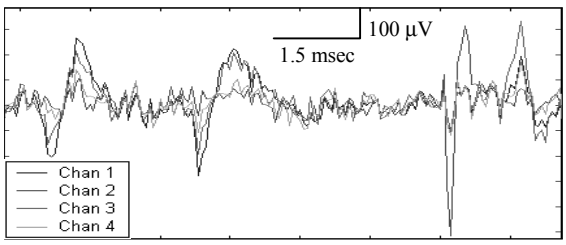

(a)

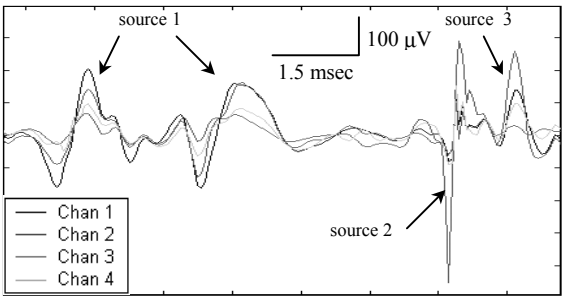

(b)

Fig. 1. (a) 4-channel experimental data. (b) Denoised signal and detection result

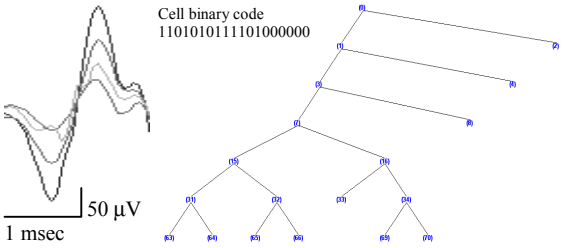

(a)

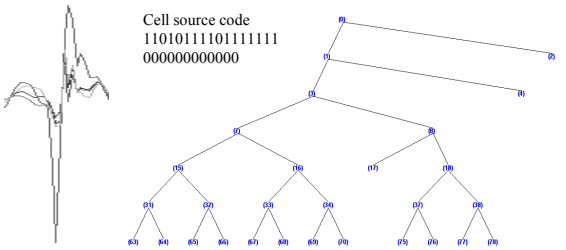

(b)

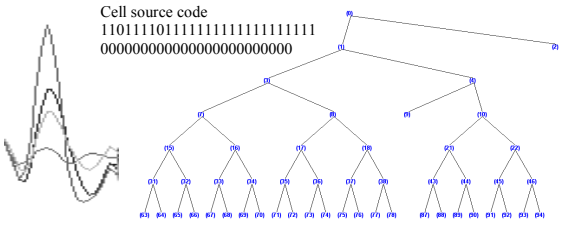

(c)

Fig. 2. Identification results for the 3 sources in Fig. 1 (L=6)

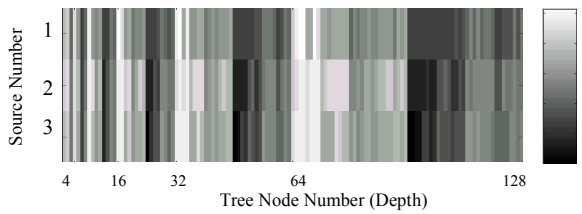

Fig. 3. Max. eigen value average along tree nodes for sources identified in Fig. 1.b